THE ASTROPHYSICAL JOURNAL, 234:768–774, 1979 December 1

SOME EFFECTS OF ACOUSTIC WAVES ON SPECTRAL-LINE PROFILES

LAWRENCE E. CRAM AND STEPHEN L. KEIL[1]
Sacramento Peak Observatory[2]
AND
PETER ULMSCHNEIDER
Institut für Astronomie und Astrophysik, Universität Würzburg
Received 1979 April 6; accepted 1979 May 9

ABSTRACT

We discuss the formation of spectral lines in the presence of short-period, nonlinear, radiatively damped acoustic waves propagating through a model of the solar atmosphere. The temperature and pressure perturbations associated with the wave strongly influence the line profile. Although their wavelength is less than the depth of the velocity response function of photospheric spectral lines, the acoustic waves produce large (> 100 ms^{-1}), short-period line shifts. Acoustic waves of sufficient amplitude to account for chromospheric heating do not significantly increase the equivalent widths of photospheric lines and therefore are probably not responsible for photospheric microturbulence.

Subject headings: line formation — line profiles — radiative transfer — Sun: atmosphere — Sun: atmospheric motions

I. INTRODUCTION

The idea that nonthermal broadening of solar spectral lines is in part due to acoustic waves is quite old. For example, Biermann (1946, 1948) proposed that the solar corona could be heated by shock dissipation of acoustic waves, and he suggested that chromospheric "turbulence" could be identified with these waves. Unno and Kawabata (1955), de Jager and Kuperus (1961), and more recently, Athay and White (1979), have even made quantitative comparisons between predicted rms velocity amplitudes and "turbulence" amplitudes inferred by spectral-line analysis. These comparisons were not based on a detailed theory of line formation in the presence of acoustic waves, and their physical basis is thus somewhat uncertain.

A number of authors have attempted to provide a theoretical explanation for the inferred nonthermal broadening of solar and stellar spectral lines. Such studies are conveniently divided into two classes: (*a*) *kinematic*, in which it is assumed that Doppler displacements due to nonthermal velocity fields are the sole perturbations of the atmosphere, and (*b*) *dynamic*, in which the temperature and pressure fluctuations associated with the velocity field are also included in the line-formation model. Kinematic models are clearly incomplete. Although they may be legitimately used as simplified models to explore aspects of line-formation theory, they should be used in the analysis of real data only if their validity has been demonstrated by recourse to a dynamical model. This caveat is ignored in most astrophysical studies of line formation.

Microturbulence is a widely used kinematic model. It assumes that the spatial scale of the motion, relative to the spatial scale over which the line is formed, is so small that an average may be made over the Doppler-shifted absorption profile before the transfer equation is solved. We call this approximation "absorption profile averaging." In performing the averaging, it is usually assumed that the velocity amplitudes have a Gaussian distribution, while the directions of motion have an angular distribution which may or may not be isotropic with respect to the vertical.

As pointed out by Oster and Ulmschneider (1973), a single acoustic wave of fixed amplitude does not have a Gaussian distribution of velocity. These authors, and Shine and Oster (1973), used absorption profile averaging with an amplitude probability distribution appropriate for a sinusoidal wave to illustrate the importance of this effect. Of course, one does not expect that acoustic waves in the solar atmosphere will have a fixed amplitude, and the amplitude distribution function will also affect the line broadening. Moreover, as noted by Kneer (1976), the spatial scale of the acoustic waves underlying this model is too great to permit absorption profile averaging.

There are several kinematic models that are not based on absorption profile averaging. The simplest of these is macroturbulence, in which the Doppler-shifted emergent profiles are subject to statistical averaging. This approach is valid only if the kinematic approximation is valid and there is no velocity gradient

[1] NAS/NRC Resident Research Associate, Air Force Geophysics Laboratory, Sacramento Peak Observatory.

[2] Operated by the Association of Universities for Research in Astronomy, Inc., under contract AST 78-17292 with the National Science Foundation.

along the lines of sight. Stochastic line-formation models of the kind described by Auvergne *et al.* (1973) and Gail *et al.* (1973) are also kinematic, and are based on an *a priori* assumption concerning the stochastic distribution of velocity along the lines of sight. Kinematic models based on sinusoidal velocity fluctuations of intermediate length scales have been considered by de Jager (1972) and Durrant (1979). In kinematic studies of non–LTE line formation, both the absorption profile and the line source function are influenced by the velocity field. Studies of this problem have been reported by Kulander (1968), Athay (1970*a*), Shine (1975), and others.

Dynamical models are much harder to construct, since changes in the source function, opacity, and line profile arising from velocity-correlated temperature and pressure fluctuations must be included. Eriksen and Maltby (1967) and Kostyk and Orlova (1972) considered dynamical models based on small-amplitude acoustic waves. The resulting line profiles were computed under the "thin line" assumption, which implies that the emergent line depression is proportional to the line absorption profile in the thin layer where the line is formed. There is no need to solve the transfer equation in this case because self-absorption is assumed to be negligible. Dynamical models in which the full transfer equation was solved at various phases of the wave have been described by Olsen (1966), who considered LTE line formation and linearized acoustic wave modes, and by Heasley (1975) and Cram (1976), who both considered non–LTE line formation and nonlinear wave models.

We believe that satisfactory understanding of solar and stellar atmospheric "turbulence" can come only with the application of dynamical models for non-thermal line-broadening processes. Spectral-line analysis per se is an extremely ambiguous procedure, so that as many constraints as possible must be imposed on the underlying atmospheric structure. Dynamical models provide such constraints, provided they are based on clearly formulated descriptions of gas-dynamical processes. This paper discusses the effects of one such dynamical process—short-period acoustic waves—on some aspects of the formation of Fe I lines in a model stellar atmosphere similar to the solar atmosphere.

II. THE MODEL

The gas-dynamical model underlying the line-formation calculations has been described by Ulmschneider *et al.* (1978). The model describes the upward vertical propagation of a train of plane acoustic waves generated by an oscillating piston, which moves sinusoidally with prescribed period P and velocity amplitude A_v. The train of waves propagates into a model atmosphere whose initial structure is that of a gray atmosphere in hydrostatic and radiative equilibrium with $T_{\rm eff} = 5800$ K and $\log g = 4.4$. As the waves propagate through the deep photosphere ($1 \lesssim \tau \lesssim 0.1$) they are strongly damped by radiation losses, again treated by a gray approximation. The motion is followed for many periods until a steady state is reached. Because the acoustic waves steepen to form shock waves and so deposit much of their wave energy into the thermal field, the quasi-steady state exhibits an outward temperature rise that may be analogous to the temperature rise of the chromosphere.

This model is, at best, a highly idealized description of the generation, propagation, and dissipation of acoustic waves in the solar atmosphere. In particular, the assumption of a gray absorption coefficient ignores the importance of line cooling in the upper photosphere and chromosphere (Athay 1970*b*; Giovanelli 1979), and the assumption of constant specific heat ignores wave energy flow between the thermal field and ionized hydrogen. Both of these deficiencies will be improved in future calculations. On the other hand, it is not clear how to modify the model to take account of such factors as oblique propagation, wave coupling, and the simultaneous existence of a distribution of wave periods, phases, and amplitudes. The gas-dynamic model is thus far from satisfactory, but it does contain much of the physics of wave propagation in the photosphere; consequently, it is instructive to compute the effects of the model on the profiles of photospheric lines.

The line-formation model is similar to that described by Keil and Canfield (1978). The transfer equation is

$$\frac{dI_\nu}{dz} = \kappa_\nu (I_\nu - S_\nu) , \tag{1}$$

where I_ν is the specific intensity at frequency ν, κ_ν and S_ν are the monochromatic opacity and source function, respectively, and z is the Eulerian depth coordinate. We have

$$\kappa_\nu = \kappa_\nu{}^L + \kappa^c \tag{2}$$

and

$$S_\nu = \frac{\kappa_\nu{}^L S_L + \kappa^c S_c}{\kappa_\nu{}^L + \kappa^c} , \tag{3}$$

where $\kappa_\nu{}^L$ and S_L are the line opacity and source function, respectively, and κ^c and S_c are the continuum opacity and source function, respectively.

As the wave propagates through the atmosphere, the opacities and source functions change in space and time. To estimate these changes it is necessary to know the values of state variables such as temperature, pressure, electron density, etc. Some of these are given directly by the gas-dynamic calculation, but others are not directly available because of the use of a simple equation of state. The unknown variables have been found by solving the LTE ionization equilibrium for an appropriate mixture of elements, using the electron temperature and total gas pressure from the gas-dynamic calculation as independent variables. Because the electronic degrees of freedom relax quickly at photospheric densities, we assume that ionization and excitation equilibria are established instantaneously. The approach is not self-consistent

since the equation of state used for the gas-dynamic calculations differs from that used to compute line formation. However, the approximations are expected to be acceptable provided we restrict our discussion to the photosphere where hydrogen is not significantly ionized.

With the results of this ionization equilibrium calculation available, the opacities and source functions are derived in the following way. The continuum source function S_c is set equal to the Planck function $B_\nu(T_e)$ evaluated at the local electron temperature. The continuum opacity κ_c is computed as the sum of contributions due to neutral hydrogen and H^- absorption, and Rayleigh and Thompson scattering. We have considered the formation of lines in the spectrum of neutral iron, using a line source function,

$$S_L = B_\nu(T_e)\frac{S_L^{\rm NLTE}}{S_c^{\rm NLTE}}, \tag{4}$$

where $S_L^{\rm NLTE}$ and $S_c^{\rm NLTE}$ are the line and continuum source functions (for the appropriate line and atmospheric depths) found by Lites (1972) in his study of non–LTE effects in a multilevel model of the Fe I atom in the solar atmosphere. Perturbations in S_L arise only from changes in $B_\nu(T_e)$: Lites's source functions are not varied. The monochromatic line absorption coefficient, ignoring stimulated emission, is

$$\kappa_\nu^L = \frac{h\nu}{4\pi} N_l B_{lu}\phi_\nu, \tag{5}$$

where N_l is the lower-level occupation number for the transition in question, B_{lu} is an Einstein coefficient, and ϕ_ν is the absorption profile. We have taken

$$\phi_\nu = \frac{1}{\sqrt{\pi}\Delta\nu_{\rm D}} H\left\{a, \frac{[\nu - \nu_0 - (\nu_0/c)v]}{\Delta\nu_{\rm D}}\right\}, \tag{6}$$

where $\Delta\nu_{\rm D}$ is the Doppler width, H is the Voigt function with damping parameter a (assumed to have the constant value 0.03), and v is the material velocity amplitude in the wave. Lites's (1972) results have been used to approximate the non–LTE effects on the occupation number N_l via

$$N_l = b_l N_l^*, \tag{7}$$

where N_l^* is the LTE occupation number and b_l the departure coefficient. Our treatment of non–LTE effects is approximate, because we do not vary the departure coefficients in the presence of the wave. However, the approximations should adequately represent non–LTE effects which are mainly due to highly nonlocal photoionization processes and, in any case, are very small for the lines considered here.

The emergent line profile at each time step of the gas-dynamic calculation was obtained by numerical quadrature of the transfer equation at many frequencies across the line. Great care was taken to ensure that rapid depth variations in the monochromatic opacity, due to large velocity gradients, were correctly integrated. Numerical tests with simple models showed that the uncertainty in the relative intensity is less than 0.1%, and in the line shifts less than 1.0%.

III. RESULTS

We discuss here the results of calculations based on a wave with period $P = 30$ s, which carries a mechanical flux of 5×10^7 ergs cm^{-2} s^{-1} into the photosphere. Approximately 90% of this flux is radiatively dissipated in the photosphere; the mechanical flux remaining when the wave passes the temperature minimum is then sufficient to provide the energy requirements for chromospheric heating (Athay 1976). The piston is located at $\tau = 3$ and moves with a velocity amplitude $A_v = 170$ ms^{-1}. The height dependence of the velocity, temperature, and pressure fluctuations in the quasi-steady state about 18 minutes (36 periods) after initialization of the wave are shown in Figure 1. The height variation of the root mean square (rms) of these fluctuations is also shown: the irregularities in the upper parts of the rms curves are artifacts due to improper averaging over the large amplitude-rapid changes associated with the shock waves. The rms velocity amplitude in the photosphere is ~ 160 ms^{-1} for $0 < h < 250$ km (above $\tau = 1$), rising to ~ 500 ms^{-1} at $h = 500$ km. The wave propagates upward with a sign convention chosen so that positive velocities are associated with compression and a blueshift of the absorption profile.

The profiles of the Fe I lines used by Keil (1979) in his study of solar granulation have been synthesized. These lines exhibit a wide range of equivalent widths and excitation potentials. Some important properties of the synthesized lines are given in Table 1. Because the gray radiative equilibrium model underlying the gas-dynamic calculations is only a rough approximation to the solar atmosphere, and because the gas-dynamic calculations themselves are highly idealized, the quantitative values in this table are less important than the trends.

For all lines studied, the mean profile obtained by averaging instantaneous profiles over one wave period is displaced redward. The displacement increases with increasing line strength, and for lines of a given strength it is larger when the lower-level excitation potential is smaller. The redshift of the point of minimum intensity is always greater than that of the center of gravity of the line. As the wave propagates through the atmosphere, the line profile changes, and characteristic measures of the line position oscillate in wavelength. The rms amplitudes of the shifts of the center of gravity and of the minimum of the profile are shown in Table 1. For the stronger lines the position of the minimum never moves blueward of the rest line center, despite the fact that the velocity oscillations in the wave are symmetric about zero.

To clarify the process of line formation in the presence of short-period acoustic waves, we consider the formation of the zero-volt line Fe I λ5166.3 in more detail. Figure 2 shows the time dependence of

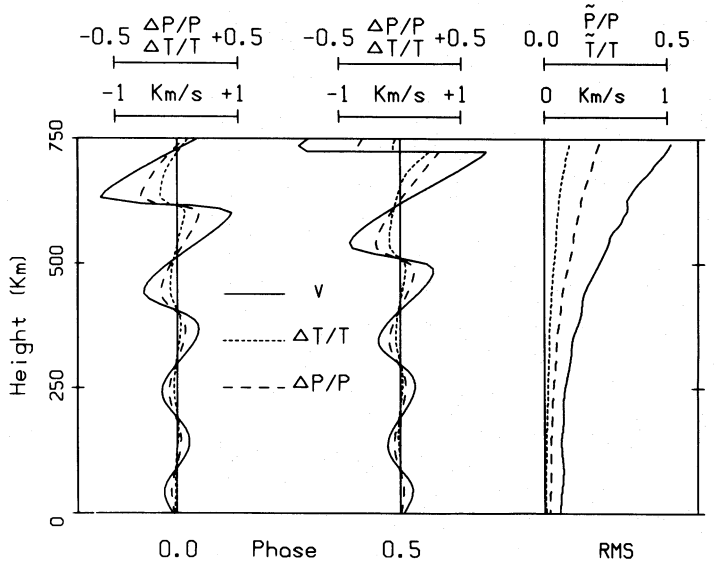

FIG. 1.—Height variation of the velocity and relative temperature ($\Delta T/T$) and pressure ($\Delta P/P$) fluctuations in the acoustic wave after a quasi-steady state has been reached. The period of the wave is 30 s and the velocity amplitude of the piston at $\tau = 3$ is 170 ms^{-1}. The height variation of the rms of these fluctuations is also shown.

the synthesized profile of this line during one complete period. The velocity, temperature, and pressure fluctuations associated with the wave have all been included. No additional nonthermal broadening has been introduced. The core of the line is always asymmetric, and the minimum of the line is always redshifted relative to the rest line center. The line center does not oscillate sinusoidally. The rms amplitude of the line center (point of minimum intensity) is 191 ms^{-1}, while the center of gravity of the line oscillates with an rms amplitude of 64 ms^{-1}.

Figure 3 exhibits the run of normalized monochromatic contribution function with depth, at various positions across the line and at opposite phases of the wave. The contribution function is defined by

$$c_\lambda = S_\lambda \kappa_\lambda \exp(-\tau_\lambda)/I_\lambda^0 , \quad (8)$$

where I_λ^0 is the emergent intensity at wavelength λ. The shapes of these curves arise from the complex interplay between fluctuations in the source function, lower-level occupation number, and absorption profile. Note that the line core is formed in the photosphere about 300 km above $\tau = 1$, and that there are conspicuous differences between the contribution functions on opposite sides of the line at (*a*) the same epoch and (*b*) times separated by half a period. The differences in case (*a*) are due solely to the effects of velocity gradients at that instant because the temperature and pressure fluctuations produce no line asymmetry. In case (*b*) the value of the absorption profile (which is symmetric about local line center) is unchanged at $+\Delta\lambda(t)$ and $-\Delta\lambda(t + P/2)$ because $v(t)$ and $-v(t + P/2)$ are almost equal in the photospheric part of the wave: the differences in this case are then due entirely to temperature and pressure fluctuations.

Figure 4 compares the line profile emitted from the initial undisturbed radiative equilibrium atmosphere

TABLE 1

OSCILLATION AMPLITUDES AND DISPLACEMENTS OF SYNTHESIZED Fe I LINES

λ (Å)	Multiplet	low EP (eV)	obs EW (mÅ)	$V_{\rm min}^{\rm rms}$ (ms^{-1})	$V_{\rm cg}^{\rm rms}$ (ms^{-1})	$\langle V\rangle_{\rm min}$ (ms^{-1})	$\langle V\rangle_{\rm cg}$ (ms^{-1})
5213.8	962	3.93	7.5	21	23	7	5
5213.4	1165	4.37	9	23	25	9	6
5178.8	1166	4.37	24	20	24	12	5
5164.6	1166	4.42	48	16	23	37	8
5165.4	1089	4.20	87	99	24	302	17
5216.3	36	1.60	108	167	48	631	47
5166.3	1	0.00	115	191	64	554	64
5215.2	553	3.25	116	161	45	401	23
5162.3	1089	4.16	154	198	30	434	25
5171.6	36	1.48	160	247	89	747	86
5167.5	37	1.48	blend	243	120	838	115

NOTE.—$V_{\rm min}^{\rm rms}$ and $V_{\rm cg}^{\rm rms}$ are the rms fluctuations of the minimum and the center of gravity; $\langle V\rangle_{\rm min}$ and $\langle V\rangle_{\rm cg}$ are the redward displacements of the minimum and the center of gravity of the mean profile.

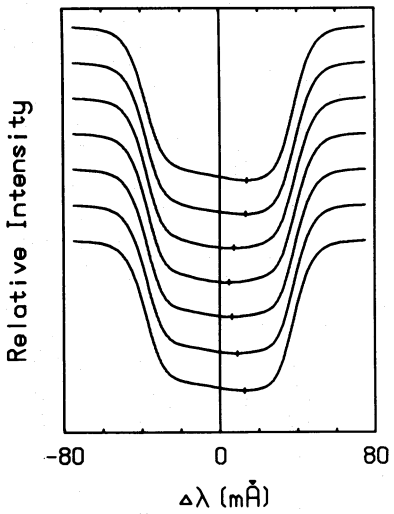

FIG. 2.—Time variation of the synthesized profile of Fe I λ5166.3, at seven equally spaced intervals beginning at 1093.3 s and spanning a full period. Tick-marks indicate the position of the minimum of the line profile.

with four models that include, in various ways, non-thermal effects. Model (1) in Figure 4 shows the effects of a typical Gaussian microturbulence model, the solar model of Lites (1972). This model decreases from ~ 2.8 km s^{-1} at $h = 0$ ($\tau = 1$) to ~ 380 ms^{-1} at $h = 400$ km, thereafter increasing into the chromosphere. These values should be compared with the thermal velocity of iron, which is 1.2 km s^{-1} at 5000 K, and with the rms velocity amplitude of the wave, as shown in Figure 1. As expected, microturbulence broadens the line and increases its equivalent width.

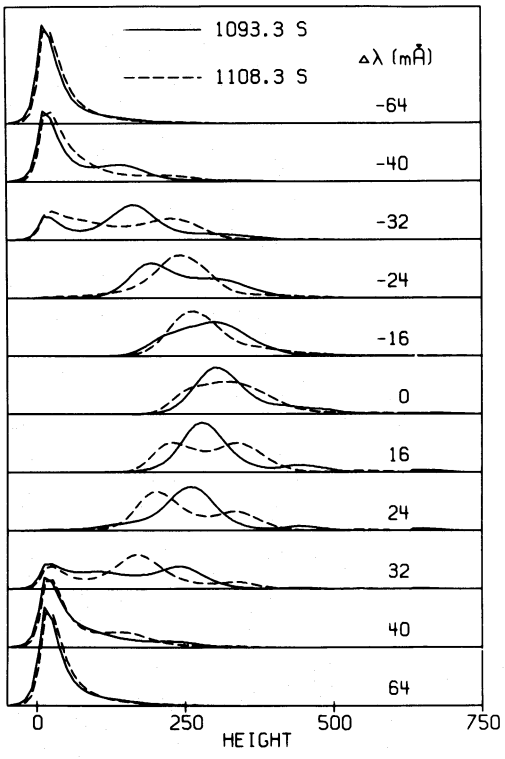

FIG. 3.—Height variation of the monochromatic contribution functions (normalized to unit area) across the line profile, at the two phases of the wave shown in Fig. 1. The corresponding line profiles are the first and fourth from the top of Fig. 2.

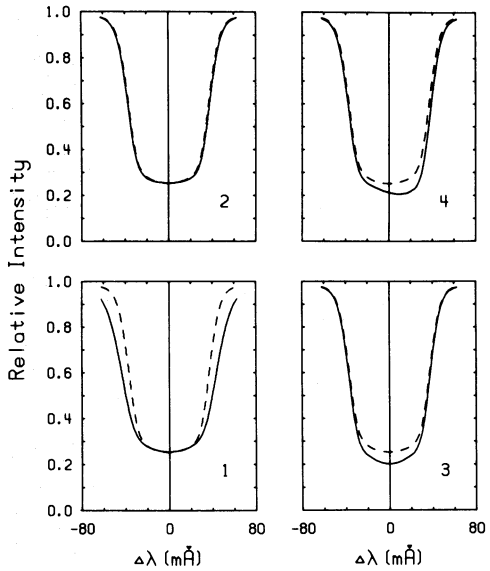

FIG. 4.—Dashed line in each panel is the synthesized line profile emitted by the initial radiative equilibrium atmosphere. The solid profiles are (1) a model including Lites's (1972) microturbulence; (2) the time average of a kinematic model including only the velocity field of the acoustic wave, and suppressing ΔT and ΔP; (3) the time average of a model including ΔT and ΔP, and suppressing the wave velocity; (4) the time average of the profiles shown in Fig. 2, with all wave fluctuations included.

Model (2) in Figure 4 shows the mean profile of a *kinematic* model that includes only the velocity field of the wave. Temperature and pressure fluctuations are artificially suppressed, and the temperature and pressure distributions of the initial atmosphere are used instead. The kinematic model produces only a small broadening of the line, the equivalent width increasing from 57.2 mÅ to 58.5 mÅ. This is expected, since the rms velocity of the wave is much smaller than the thermal velocity of iron. The rms line shifts of the time-dependent profiles that lead to this mean profile are 26 ms^{-1} at the minimum intensity point and 23 ms^{-1} at the center of gravity. Again, this result is expected from a kinematic calculation because the wave has a small wavelength relative to the depth of the layer in which the line is formed.

Model (3) in Figure 4 shows the mean profile that is produced when the velocity field is suppressed while the temperature and pressure fluctuations remain in the line synthesis. Although this model is quite artificial, it does illustrate the importance of temperature and pressure fluctuations in determining the mean emergent radiation. A model atmosphere inferred from this mean profile would be cooler than the initial atmosphere at corresponding optical depths. This trend agrees with the change in the temporal mean of the temperature fluctuations themselves

(Ulmschneider *et al.* 1978, Fig. 6), but we defer a detailed comparison to a future study which will also synthesize the continua.

Model (4) in Figure 4 shows the mean profile produced when the velocity, temperature, and pressure fluctuations are all included in the synthesis. This case is the temporal average of the profiles shown in Figure 2. A comparison of models (4) and (2) in Figure 4 shows the overwhelming importance of including *dynamical* effects in any study of line formation in the presence of short-period acoustic waves. In this case the kinematic model is totally inadequate.

Inspection of Figures 1, 2, and 3 will show the difficulty of identifying a dominant physical effect when the self-consistent problem is being considered. To gain insight into the line-formation mechanism we have therefore artificially isolated the separate physical processes by suppressing the effects of temperature and pressure fluctuations in all but one quantity. In this way we have identified the temperature sensitivity of the Fe I–Fe II ionization equilibrium as the dominant process in the formation of λ5166.3. In compressed parts of the wave, the temperature is elevated and the population of Fe I falls markedly, despite the increase in gas pressure and electron pressure. Thus the compressive parts of the wave are relatively transparent, and the line of sight passes preferentially into the cool, expansive parts of the wave where the absorption profile is redshifted. The effect is more important for strong lines because they are formed above the region where radiative damping holds down the temperature fluctuations, and for lines whose lower level has a small excitation potential because the level population is a more sensitive function of temperature in this case (Fe I being the minority ionic state).

IV. DISCUSSION

These results may be summarized as follows: (1) short-period acoustic waves with an amplitude sufficient to account for chromospheric heating do not make a significant contribution to photospheric microturbulence, as would be inferred from studies of the curve-of-growth or line-profile shapes; and (2) the pressure and temperature fluctuations associated with the velocity field of the acoustic wave may modify the line-formation process to such an extent that the kinematic approximation is completely inadequate. The quantitative effect depends on the actual line in question, and can be estimated only by solving the appropriate dynamical problem.

The second result has several important consequences, both on the inference of atmospheric velocity fields from spatially and temporally resolved observations of line shifts and on studies of the shifts and asymmetries of mean solar line profiles. In discussing the resolved observations it is useful to introduce the concept of a *velocity transfer function* T_v defined by

$$T_v = \frac{V(\text{obs})}{V(\text{true})} . \tag{9}$$

Here, V(obs) is a statistic (such as the rms) of the observed Doppler shift (in velocity units) of some characteristic property of a line profile (point of minimum intensity, center of gravity, line bisector at a specified residual intensity, lambda meter response, etc.), and V(true) is a corresponding statistic of the nonthermal velocity amplitude in a specified region of the atmosphere. The value of T_v for a specified statistic depends on the line characteristic that is measured, on the region referred to in V(true), on the dynamical origin of the velocity field under consideration, and on external factors such as the atmospheric seeing at the time of observation.

The transfer function for rms velocity amplitudes, T_v^{rms}, in the presence of waves has been discussed by Mein (1971), de Jager (1972), and Durrant (1979), who refer to it as a "gain" or "filter" function. These authors have used kinematic models to quantify situations intermediate to the obvious limits $T_v^{\text{rms}} \to 1$ for waves with a wavelength much longer than the depth over which the line is formed, and $T_v^{\text{rms}} \to 0$ for waves with extremely short wavelengths. The results, for idealized atmospheres not unlike that considered here, yield T_v^{rms} as a function of kH, the product of the vertical wavenumber of the wave k and the continuum opacity scale height H. For λ5166.3 and the present model atmosphere, $k \approx 2\pi/220\ \text{km}^{-1}$ and $H \approx 65$ km, so that $kH \approx 1.9$. For this value the kinematic models predict $T_v^{\text{rms}} \approx 0.17$ for measurements referring to the position of the line bisector (Durrant 1979, Fig. 4). With this transfer function and an rms wave-velocity amplitude of $160\ \text{ms}^{-1}$ (Fig. 1), we expect to observe rms line shifts of the order of $27\ \text{ms}^{-1}$. This is confirmed by the kinematic calculations of the effects of the wave. But the full dynamic calculations predict rms line-center fluctuations of $191\ \text{ms}^{-1}$, or a transfer function $T_v^{\text{rms}} \sim 191/160 \sim 1.2$, which is 7 times the kinematic value. The center of gravity of the line (which is more readily measured) oscillates with a smaller amplitude, but the transfer function for this line property is still $T_v^{\text{rms}} \sim 64/160 \sim 0.4$, which is approximately 2.4 times the kinematic prediction.

The transfer function for short-period acoustic waves must be known to interpret the high-frequency power seen in power spectra of observed solar line shift observations (Deubner 1976; Keil 1979). Deubner's (1976) observations reveal power (above the noise level) for all periods longer than ~20 s, and in certain lines the power spectrum exhibits a pattern of maxima and minima. Deubner used a kinematic model to interpret the observed maxima and minima as fringes resulting from constructive or destructive interference between the velocity-wave and the velocity-response function of the line. Durrant (1979), on the other hand, suggested that the structure of the power spectrum arises from interference between the aperture of the measuring device and the intensity fluctuations across the line profile. The present study shows that both of these explanations are oversimplified because the temperature and pressure fluctuations associated with short-period acoustic

waves should not be ignored in line-formation studies.

Because Deubner's (1976) observations were made on photographic negatives with a lambdameter, his measurements refer to the line core where, as we have seen, the transfer function derived from kinematic studies may be as much as a factor of 7 too small. It is possible, therefore, that Deubner's derived atmospheric-velocity amplitudes are much too large, and that the consequent estimate of mechanical energy flux is more than 50 times too large. If this is so, then the inferred atmospheric-velocity amplitudes are in rough agreement with the energy requirements for chromospheric heating, but too small to account for photospheric microturbulence.

Our results are also of interest to studies of the shifts and asymmetries found in spatially and temporally averaged observations of solar spectral lines. Asymmetry is generally measured by drawing the bisector of the line profile: this bisector usually has a "C-shape," with the core of the line and the extreme wings both redshifted by several mÅ relative to the bisector at the half-intensity point. Observations and suggested explanations of these asymmetries have been summarized by Magnan and Pecker (1974). Our calculated profiles suggest that acoustic waves may be responsible for most of the asymmetry described by the lower part of the C-shape.

Acoustic waves also lead to a displacement of the mean line relative to the rest wavelength. Observations of the Sun show that, when corrected for the gravitational redshift, photospheric spectral lines are shifted blueward at disk center (by about 300 ms^{-1}, depending on line strength, excitation potential, and method of measuring the line shift); this shift becomes progressively smaller toward the limb, and beyond $\mu \sim 0.2$ the shift is redward of the rest wavelength. The observations have been summarized by Beckers and Nelson (1978), who have shown that most features of the observations can be explained qualitatively by intensity/line-shift correlations in the solar granulation. Our calculations show that short-period acoustic waves will produce a significant, but not dominant, displacement of averaged photospheric line profiles at disk center (toward the red). Their effect at the limb cannot be reliably estimated without a model for the angular distribution of the acoustic wave field.

V. CONCLUSIONS

Our principal conclusion is that the temperature and pressure fluctuations associated with velocity fields must not be ignored in studies of line formation in the presence of short-period acoustic waves. Velocity-correlated temperature and pressure fluctuations will certainly occur in all other dynamical processes acting in the solar atmosphere, and they can be ignored only if detailed line-synthesis studies based on full dynamical models show that the kinematic approximation is acceptable.

We have shown that short-period acoustic waves carrying sufficient energy flux to heat the solar chromosphere are not major contributors to photospheric microturbulence. A dynamical model for microturbulence still eludes us. The velocity-transfer function for short-period acoustic waves may be greatly underestimated by a kinematic model. Fortunately, this implies that observations of short-period line shifts of the kind made by Deubner (1976) and Keil (1979) will provide a reliable picture of the spectrum, amplitude, and angular distribution of short-period acoustic waves in the solar atmosphere.

We thank Dr. C. J. Durrant for many helpful discussions.

REFERENCES

Athay, R. G. 1970*a*, *Solar Phys.*, **12**, 175.
———. 1970*b*, *Ap. J.*, **161**, 713.
———. 1976, *The Solar Chromosphere and Corona* (Dordrecht: Reidel).
Athay, R. G., and White, O. R. 1979, *Ap. J.*, **226**, 1135.
Auvergne, M., Frisch, H., Frisch, U., Froeschlé, Ch., and Pouquet, A. 1973, *Astr. Ap.*, **29**, 93.
Beckers, J. M., and Nelson, G. D. 1978, *Solar Phys.*, **58**, 243.
Biermann, L. 1946, *Naturwissenschaften*, **33**, 118.
———. 1948, *Zs. Ap.*, **25**, 161.
Cram, L. E. 1976, *Astr. Ap.*, **50**, 263.
de Jager, C. 1972, *Solar Phys.*, **25**, 71.
de Jager, C., and Kuperus, M. 1961, *Bull. Astr. Inst. Netherlands*, **16**, 71.
Deubner, F.-L. 1976, *Astr. Ap.*, **51**, 189.
Durrant, C. J. 1979, *Astr. Ap.*, **73**, 137.
Eriksen, G., and Maltby, P. 1967, *Ap. J.*, **148**, 833.
Gail, H. P., Hundt, E., Kegel, W. H., Schmidt-Burgk, J., and Traving, G. 1973, *Astr. Ap.*, **32**, 65.
Giovanelli, R. G. 1979, *Solar Phys.*, **59**, 293.
Heasley, J. N. 1975, *Solar Phys.*, **44**, 275.
Keil, S. L. 1979, *Ap. J.*, submitted.
Keil, S. L., and Canfield, R. C. 1978, *Astr. Ap.*, **70**, 169.
Kneer, F. 1976, in *Interpretation of Atmospheric Structure in the Presence of Inhomogeneities*, ed. C. J. Cannon (Sydney: University of Sydney Press), p. 29.
Kostyk, R. I., and Orlova, T. V. 1972, *Solar Phys.*, **26**, 42.
Kulander, J. 1968, *J. Quant. Spectrosc. Rad. Transf.*, **8**, 273.
Lites, B. 1972, Ph.D. thesis, University of Colorado.
Magnan, Ch., and Pecker, J.-C. 1974, *Highlights of Astronomy*, **1**, 171.
Mein, P. 1971, *Solar Phys.*, **20**, 3.
Olsen, E. C. 1966, *Ap. J.*, **143**, 904.
Oster, L., and Ulmschneider, P. 1973, *Astr. Ap.*, **29**, 1.
Shine, R. A. 1975, *Ap. J.*, **202**, 543.
Shine, R. A., and Oster, L. 1973, *Astr. Ap.*, **29**, 7.
Ulmschneider, P., Schmitz, F., Kalkofen, W., and Hammer, R. 1978, *Astr. Ap.*, **70**, 487.
Unno, W., and Kawabata, K. 1955, *Pub. Astr. Soc. Japan*, **7**, 21.

LAWRENCE E. CRAM and STEPHEN L. KEIL: Sacramento Peak Observatory, Sunspot, NM 88349

PETER ULMSCHNEIDER: Institut für Astronomie und Astrophysik, Am Hubland, D-8700 Würzburg, Federal Republic of Germany